Hindawi
Computational Intelligence and Neuroscience
Volume 2022, Article ID 8906838, 10 pages
https://doi.org/10.1155/2022/8906838

Research Article

Computational Intelligence Powered Performance Analysis on Phase Change Heat Storage Air Source Heat Pump System

Caihong Yin,[1] **Ronghua Wu**,[2,3] **Hao Zhan**,[3] **Hao Yu**,[2] **and Changqing Liu**[3]

[1]*Jiaozhou Bureau of Science, Technology and Industrial Information, Qingdao, Shandong 266399, China*
[2]*Qingdao Kechuang Blue New Energy Co., Ltd, Qingdao, Shandong 266300, China*
[3]*College of Mechanical and Electrical Engineering, Qingdao University, Qingdao, Shandong 266071, China*

Correspondence should be addressed to Ronghua Wu; wuronghua18@126.com

Received 21 May 2022; Revised 8 July 2022; Accepted 14 July 2022; Published 4 August 2022

Academic Editor: Shahid Mumtaz

Aiming at the performance deterioration of air source heat pump at low temperature in cold area, an air source heat pump system with sodium chloride aqueous solution as low temperature phase change heat storage material was proposed to increase the air inlet temperature of the unit under low temperature conditions and improve the low temperature performance of the heat pump unit. The system form, unit energy consumption model, and economic model were given, and the operating economy of the traditional electric auxiliary heat air source heat pump system and the phase change heat storage air source heat pump system were compared through computational intelligence powered methods. On this basis, the operation economy of the heat pump system using different concentrations of sodium chloride solution as the heat storage material was simulated and optimized, and the operation efficiency and energy-saving performance of the system were analyzed by taking an actual residential building in a cold area as an example. The simulation results showed that the Heating Seasonal Performance Factor (HSPF) of the heat pump system using 8.5% sodium chloride aqueous solution as the heat storage material is 2.24, and the HSPF of the traditional electric auxiliary heat pump system is 1.83. Compared with the traditional electric auxiliary heat pump system, the phase change heat storage heat pump system saves heating energy consumption by 19.6% and defrosting energy consumption by 38.8%. The heat pump system using 10% sodium chloride aqueous solution as the heat storage material has the best operating economy, and the system HSPF is 2.33, which saves heating energy consumption by 23.2% and defrosting energy consumption by 34% compared with the traditional heat pump system. The operation condition of phase change heat storage air source heat pump system is stable, and the system performance is significantly improved.

1. Introduction

Air source heat pump is widely used in building heating and domestic hot water supply from renewable air. Heat pump takes heat from low temperature heat source based on the inverse Carnot cycle, and its condensation temperature is related to building heating requirements. In recent years, the promotion of energy-saving buildings reduces the heat standard for heating, but in order to ensure better heating comfort and heat transfer efficiency, the water supply temperature of radiant floor heating is still recommended to remain above 40°C [1]. The evaporation temperature of the heat pump changes with the outdoor temperature and maintains a certain degree of superheat. When the evaporation temperature decreases due to the decrease of the outdoor temperature, the compressor needs to consume more electrical energy to improve the compression ratio to keep the condensation temperature constant, and both the heating capacity and COP of the heat pump will be significantly attenuated at lower ambient temperature [2].

Scholars in various countries have done a lot of research on improving the low temperature performance of air source heat pump and put forward a variety of solutions, which mainly focus on the structural improvement of the heat pump itself and the coupling of multiple heat sources in two aspects. The structural improvement of air source heat pump system operating in cold regions includes exploring new technologies and applying new working medium. Ji et al. [3]

conducted an experimental study on the heating performance of a two-stage variable speed scroll compressor jet assisted air source heat pump, and the results showed that when the ambient temperature was reduced to −20°C, the system was still able to achieve 68.1% of the nominal working condition, and it could operate stably in severe cold regions. Lx et al. [4] experimentally verified the operational stability of the cascade air source heat pump system when it was applied in cold regions, and the results showed that the system operated stably in the heating season, and the efficiency was much higher than that of the gas boiler. Wu et al. [5] proposed and theoretically validated a new H_2O/ionic liquid absorption and CO_2 compressed air source heat pump system for ultra-low ambient temperature, which operated well at −30°C ambient temperature, and the primary energy efficiency (PEE) was higher than 1.256. Zhang et al. [6] simulated the heating performance of the cascade air source heat pump system using R134a/CO_2 in severe cold regions. The simulation results showed that the HSPF of the system in the heating season remained above 2.1, and the system had high economy and reliability.

Compared with the traditional air source heat pump heating system, the design and control technology of the heat pump unit with two-stage compressor and cascade system are still not mature [7], and the operating efficiency at room temperature is far lower than that of the conventional heat pump unit. The promotion of new low-temperature working materials such as CO_2 is limited due to the low unit heat load and high requirements for pressure vessels. At present, engineering applications more often use multiple heat sources coupled heating methods to reduce the operating time of heat pump units under unfavorable operating conditions. Sager and Poirier [8] conducted a field evaluation of the performance and cost competitiveness of a dual-source solar-assisted air source heat pump in cold climate, and the results showed that the system operated stably in cold climate, effectively reduced carbon emissions, and shortened the payback period. Sun et al. [9] combined electric boiler with air source heat pump to reduce the heating load of air source units in severe cold climate by peak shaving of electric boiler. The actual heating area of the system was 130650 m^2, and the heating equipment operated stably. Zhao et al. [10] designed a gas-air dual-source heat pump to replace the existing gas boiler. When the ambient temperature decreases, and the electrical price ratio of the equivalent heating capacity is lower than 0.45, the unit takes heat from natural gas, which can effectively reduce the energy consumption of heating. In addition, there are also projects that deploy air source heat pump and water source heat pump at the same time to adjust the unit load ratio according to the outdoor temperature, with good energy saving effect [11].

Heat storage technology can realize the transfer of heat in time and space. Adding heat storage system to air source heat pump system can further shorten the operation time of the heat pump under unfavorable working conditions and improve the low temperature performance of the unit. Chen et al. [12] conducted an experimental study on solar-air source heat pump system with heat storage device, and the results showed that the utilization of solar heat storage for heating at cold night could reduce the heating demand for the unit and effectively reduce the energy consumption of the unit. The COP of the system in extreme weather was maintained above 1.7. Different from most studies that directly applied solar energy heat to heat storage, Zhang et al. [13] used solar energy to preheat the cold air entering the evaporator. By increasing the dry-bulb temperature of the air and reducing the moisture content of the air, the evaporation temperature of the unit was increased, and the frosting was delayed. The system also paralleled the electric heating device behind the solar collector to preheat the air at night when the ambient temperature was low. The results showed that the system reduced the operation cost by 66.3%, resulting in significant energy saving effect. On the basis of the above system, Xu et al. [14] eliminated the electric heating device and replaced it with a heat storage tank after the condenser of the system. The unit operated at full load in the daytime and stored the surplus heat through the tank for nighttime heating, so that the unit did not operate or operated less at night, reducing the energy consumption of the unit, and reducing the number of units and unit investment.

Common heat storage technologies include sensible heat storage, latent heat storage, and electrochemical heat storage, among which latent heat storage has high heat storage density, small footprint, and stable chemical properties, which has become a hot research topic in recent years [15]. The heat storage technology based on heat pump system includes condensation side heat storage and evaporation side heat storage. The most commonly used condensation side heat storage material is paraffin [16], which is chemically stable and relatively inexpensive, with stable crystallization and no supercooling problem compared with hydrated salt [17]. The heat storage temperature of the evaporation side is generally below 0°C, which is lower than the freezing point temperature of water. Therefore, most of the ice with low cost and high heat storage density is used as the heat storage material. The melting point temperature of the solution can be flexibly changed by adding inorganic salts or organic solutes to the water. Since the freezing of salt solution has the characteristics of water molecules precipitation and then solidification, the heat storage density of fluidized ice formed by mechanical stirring and other measures is high, and the heat transfer coefficient is much higher than that of ordinary solid ice. Sidqy et al. [18] proposed a process for making ice slurry from saline seawater by scraper method. Lee and Kim [19] produced an ice slurry heat storage device with mass density of 25% by adding 6.5% ethylene glycol solution into water. Sasaki [20] applied this property to the heat storage of distribution refrigerator and achieved good results.

Adding new heat sources to the existing air source heat pump heating projects is not easy to achieve, and most regions do not have the conditions of applying water source heat pump and industrial waste heat. Adding electric boilers and gas boilers is not in line with the concept of energy saving and environmental protection, so it is difficult to get government approval. Solar air preheating can effectively reduce the operation time of the unit under adverse conditions, but large-scale utilization of solar energy needs to lay

a large area of collectors, and most old projects do not have implementation conditions. Therefore, based on not changing the old conventional air source heat pump module as much as possible, this paper proposes an air source heat pump system that uses the fluidized ice heat storage technology to store end heat for preheating cold air entering the evaporator in extremely cold weather. The heat is stored when the thermal efficiency of the unit is high in rising temperatures and released when the thermal efficiency of the unit decreases in extremely cold weather, ensuring that the unit always maintains a low compression ratio, reducing the heating energy consumption and, at the same time, reducing the investment in peak heat spare units. The system form, unit energy consumption model, and the economic model were given in the paper. The operating characteristics of the traditional air source heat pump system and the new heat pump system were compared by means of numerical analysis. On this basis, the operating economy of the heat pump system with different heat storage temperatures was simulated and optimized. Taking a residential building heating project in Dalian as an example, the system performance of the traditional heat pump heating and the new heat pump heating was compared by means of numerical analysis, and the optimal operating point of the system running in the residential area was found.

2. Introduction of Phase Change Heat Storage Air Source Heat Pump System

Since the design of the existing air source heat pump unit has been extremely mature, in order to adapt widely to the existing air source heat pump units, the phase change preheating system preheats the air by extending the air duct and then adding part of finned heat exchanger tubes at the bottom of evaporator without changing the existing structure of heat pump units and influencing the fluorine circuit cycle. When the air temperature is high, and the operating efficiency of the unit is high, such as during the day, the intermediary water is used to take heat from the end to melt the ice crystals in the heat storage device, so as to achieve the purpose of heat storage. When the outdoor temperature is low, and the unit efficiency is reduced, for example, at night, the intermediate water takes heat from the heat storage device to preheat the evaporator intake to improve the low-temperature performance of the unit. The schematic diagram of the system is shown in Figure 1.

When the outdoor temperature is low, and the operating efficiency of the air source heat pump unit decreases, open solenoid valve 1 and solenoid valve 3, and close solenoid valve 2. The intermediate antifreeze takes heat from the heat storage device through the intermediate pump and uses the finned heat exchanger tube to heat the intake air, improves the operating conditions of the unit under low ambient temperature, and increases the heating capacity of the unit.

When the outdoor temperature warms up, and the energy efficiency of the unit is high, close solenoid valve 3, open solenoid valve 1 and solenoid valve 2, and heat is taken from the intermediate water at end by the end pump, which is used for ice melting and heat storage.

Electric auxiliary heating air source heat pump system uses electric boiler as auxiliary heat source and provides heat by parallel connection of conventional air source heat pump unit and electric boiler. The outdoor design temperature of air source heat pump unit is −10°C. Start the electric boiler when the outdoor ambient temperature is lower than −10°C. It serves as the supplementary heat source after attenuation of heat generation of heat pump system under low temperature conditions.

Figure 2 is the typical air enthalpy and humidity diagram of the two heating methods. The curve ABC represents the change of air enthalpy and humidity on the surface of the evaporator fins of the conventional heat pump unit. During the process from A to B, the sensible heat of outdoor air releases heat, and the moisture content increases, while the temperature decreases. When the outdoor air reaches the state point B, it reaches the saturated humidity. From B to C, the air temperature gradually decreases, and the water vapor in the air continuously precipitates and condenses, condensing and frosting on the surface of the evaporator [21]. There are both sensible and latent heat release in this process.

The curve DEF represents the change of air enthalpy and humidity on the surface of evaporator fins of the regenerative air source heat pump unit when the heat accumulator releases heat. During the process from D to E, the air flows through the preheating fins to absorb heat, and the temperature rises. Because there is no mass transfer process in the wall-type heat exchange, the moisture content of the air will not change, and the actual moisture content of the air will decrease. During the process from E to F, the air flows through the fluorine path fins, the temperature decreases, and the moisture content increases, but it does not reach the saturated moisture content of point F. There is only sensible heat exchange in the entire heat exchange process, and there is no risk of frosting.

3. Energy Consumption Model of Air Source Heat Pump

In order to further analyze the low temperature performance of the phase change heat storage heat pump system, an energy consumption model of air source heat pump was established [22]. In the heating season, the outdoor performance balance point temperature of −10°C is selected as the design temperature [23], and the condensation temperature of the unit is 50. The operating range of a certain brand of scroll heat pump unit using R410A as the working medium is shown in Figure 3. The compressor rated suction and discharge capacity is 0.394 kg/s. According to the operating range provided by the manufacturer, the conventional heat pump unit cannot work normally when the evaporation temperature is lower than −15°C.

As a pressure regulating component, the state change of the refrigerant in the compressor is a transient process, Therefore, it is assumed that (1) the state of the refrigerant in the compressor is independent of the time constant [24], and its change process can be ignored compared with that in the heat exchanger; (2) the compression process of the refrigerant in compressor is isentropic [25]. Therefore, the steady-

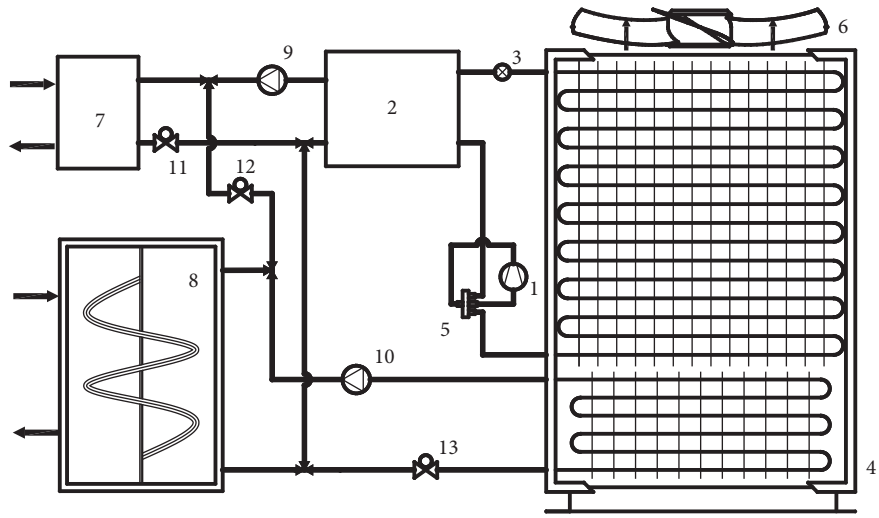

Figure 1: Operating principle diagram of phase change heat storage air source heat pump system. (1) Compressor. (2) Condenser. (3) Throttle valve. (4) Evaporator. (5) Four-way valve. (6) Fan. (7) End heat exchanger. (8) Phase change heat storage device. (9) End pump. (10) Intermediate pump. (11) Solenoid valve 1. (12) Solenoid valve 2. (13) Solenoid valve 3.

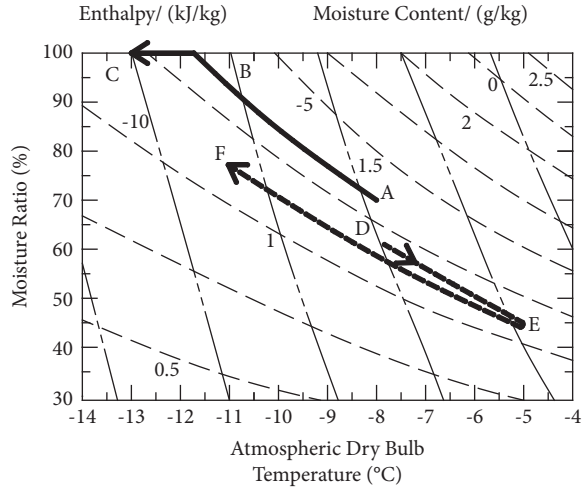

Figure 2: Air enthalpy and humidity diagram in the evaporator.

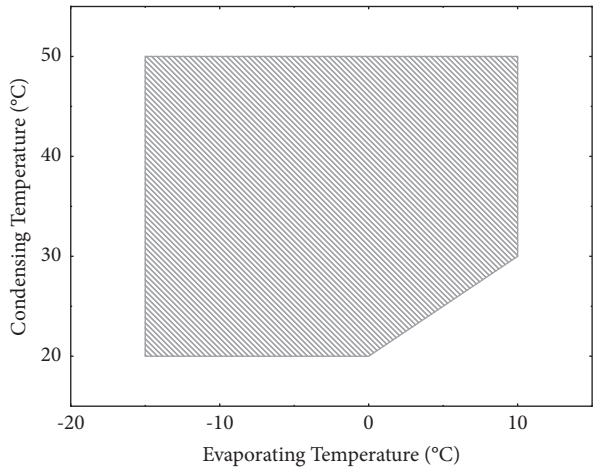

Figure 3: Compressor operating range.

state characteristics of the unit can be used instead of dynamic characteristics. The performance parameters such as the power consumption and heating capacity of the compressor are affected by evaporating temperature and condensing temperature. According to the actual operating parameters of the compressor, the Coefficient of Performance (COPcomp) curve of its operating energy efficiency can be obtained as follows:

$$\%\ \mathrm{COP}_{\mathrm{comp}} = 7.3562 + 0.09181\left(t_{\mathrm{air}} - t_{\mathrm{sh}}\right) - 0.09716\left(t_{\mathrm{c}} + t_{\mathrm{sc}}\right), \tag{1}$$

where t_{air} is the intake air temperature, °C; t_{sh} is the degree of superheat, °C; t_c is the unit outlet water temperature, °C; t_{sc} is the degree of supercooling, °C.

According to the product sample book, the rated water flow of the selected air-cooled heating module is 22.4 m^3/h, the total air volume of the fan is 48000 m^3/h, and the pump power P_{aspw} and the fan power P_{aspa} are

$$P_{\mathrm{aspw}} = \frac{G_w g \rho H}{3600 \eta_{\mathrm{pw}}},$$
$$P_{\mathrm{aspa}} = \frac{Q_{\mathrm{air,in}} P_{\mathrm{air}}}{3600 \eta_{\mathrm{pa}}}, \tag{2}$$

where G_w is the water flow rate of unit, m^3/h; g is the acceleration of gravity, 9.8 $\mathrm{m/s}^2$; ρ is the fluid density, kg/m^3; H is the head, m; η_{pw} is the pump efficiency, 0.85; $Q_{\mathrm{air,in}}$ is the intake air volume, m^3/h; P_{air} is the total pressure, kPa; η_{pa} is the full pressure efficiency, 0.85.

The unit adopts the hot gas bypass method of four-way valve reversing for defrosting [26]. According to the research results of Qu et al. [27], the energy consumption of melting and defrosting accounts for about 15.7% of the energy consumption of defrosting [27], and the evaporation of water for melting and defrosting is about 13% [28]. The defrosting energy consumption of the unit P_{def} is

$$P_{\text{def}} = \frac{Q_{\text{air}}\left(d_{\text{air,in}} - d_{\text{air,out}}\right)}{565200}\gamma, \tag{3}$$

where $d_{\text{air,in}}$ is the average moisture content of the intake air, g/m^3; $d_{\text{air,out}}$ is the average moisture content of the exhaust gas, g/m^3; γ is the coagulation heat of water, kJ/kg.

Under low temperature conditions, the heating capacity of the heat pump unit is used to meet the building heat load demand. After the ambient temperature is increased, part of the heating capacity of the heat pump unit is used for ice melting and heat storage of the heat storage device. The actual heating energy consumption P_{asp} of the unit is

$$P_{\text{asp}} = P_{\text{aspw}} + P_{\text{aspa}} + P_{\text{def}} + \frac{\left(q_{\text{load}}/\eta_{\text{asp}}\right) + \left(q_{\text{PCM}}/\eta_{\text{PCM}}\right)}{\text{COP}_{\text{comp}}}, \tag{4}$$

where q_{load} is the building heat load corresponding to ambient temperature, kW; q_{PCM} is the heat storage load, kW; η_{asp} is the unit heat transfer efficiency, 0.95; η_{PCM} is the heat storage heat transfer efficiency, 0.9.

4. Energy Consumption Model of Phase Change Heat Storage Device

The phase change heat storage device adopts the ice crystal cold storage technology of dynamic crystallization [29, 30], and the heat exchange area on both sides is 20 m^2. Dynamic crystallization overcomes the problems of high supercooling degree, wall thermal resistance increasing with the amount of ice and ice blockage of pipeline existing in traditional static ice storage technology. The phase change heat storage material is a certain concentration of sodium chloride salt solution, and a mechanical stirring structure is set inside the device to ensure that the subcooling degree of the salt solution is consistent, so that the freezing process occurs homogeneously. Adjusting the mass concentration of sodium chloride in the solution can change the temperature of the phase transition point of the device (supercooled crystallization temperature of sodium chloride solution), and the approximate formula [31] of the crystallization point temperature T_{crys} of sodium chloride aqueous solution is

$$T_{\text{crys}} = -36.97w^2 - 57.28w + 0.1037, \tag{5}$$

where w is the mass concentration of sodium chloride, %.

The partially crystallized sodium chloride solution is in a two-phase flow state in the device and has high fluidity [32]. Compared with the traditional static ice storage technology, the ice crystal cold storage can realize the continuous crystallization of the cold storage device, and the ice crystal in the solution has a higher specific surface area for heat exchange. The heat transfer coefficient of ice slurry with ice content of 5w%~30w% is about 3 kW/(m^2·K), and the heat of solution is about 334 kJ/kg. In order to simplify the calculation process, the following assumptions are made for the phase change heat storage process: (1) the pressure drop and heat loss of intermediary water in the regenerator are ignored in the modeling process; (2) intermediate water flows in all directions in the heat accumulator; (3) the equivalent specific heat capacity method is used to describe the phase transition process of phase change materials [25]. Based on the above assumptions, the heat transfer process of the phase change side of the accumulator is as follows:

$$\begin{cases} E_{\text{PCMch,sc}} \displaystyle\int_0^{\tau_{ch}} k_{\text{PCM,sc}} A_{\text{PCM,sc}}\left(t_{\text{ave,sc}} - t_{\text{PCM,sc}}\right)\text{d}\tau, \\ E_{\text{PCMch,pc}} \displaystyle\int_0^{\tau_{ch}} k_{\text{PCM,pc}} A_{\text{PCM,pc}}\left(t_{\text{ave,pc}} - t_{\text{PCM,pc}}\right)\text{d}\tau, \\ E_{\text{PCMch,cc}} \displaystyle\int_0^{\tau_{ch}} k_{\text{PCM,cc}} A_{\text{PCM,cc}}\left(t_{\text{ave,cc}} - t_{\text{PCM,cc}}\right)\text{d}\tau, \end{cases} \tag{6}$$

where E_{PCMch} is the heat storage of phase change material, kJ; k_{PCM} is the heat transfer coefficient of phase change side, W/(m^2·K), calculated according to Dittus-Boelter formula; A_{PCMch} is the heat transfer area on phase change side, m^2; t_{ave} is the average temperature of tube wall, ˚C; t_{PCM} is the average temperature of phase transition side, ˚C; τ_{ch} is the heat storage time, h; subscript: sc is the overheating stage; pc is the two-phase stage; cc is the supercooling stage.

Intermediate side heat transfer process:

$$E_{\text{tr,in}} = m_{\text{tr}}\left(h_{\text{tr,out}} - h_{\text{tr,in}}\right) = k_{\text{tr}} A_{\text{tr}}\left(t_{\text{tr,out}} - t_{\text{tr,in}}\right), \tag{7}$$

where $E_{\text{tr,in}}$ is the heat storage capacity, kW; m_{tr} is the intermediate water flow, kg/s; $h_{\text{tr,out}}$ is the outlet enthalpy, kJ/kg; $h_{\text{tr,in}}$ is the inlet enthalpy, kJ/kg; k_{tr} is the heat transfer coefficient of intermediate water side, kW/(m^2·K); A_{tr} is the heat exchange area of intermediate water side, m^2; $t_{\text{tr,out}}$ is the outlet water temperature, ˚C; $t_{\text{tr,in}}$ is the inlet water temperature, ˚C.

The energy consumption of phase change heat storage device is

$$P_{\text{PCM}} = P_{\text{PCM,motor}} + q_{\text{PCM}}\left(1 - \eta_{\text{PCM}}\right), \tag{8}$$

where $P_{\text{PCM,motor}}$ is the motor power, kW.

The finned tube side adopts traditional dry air-cooled finned heat exchanger, and the heat exchange $E_{\text{fin,evap}}$ is

$$E_{\text{fin,evap}} = m_{\text{fin}}\left(h_{\text{fin,in}} - h_{\text{finout}}\right) = k_{\text{fin}} A_{\text{evap}}\left(t_{\text{fin,in}} - t_{\text{fin,out}}\right), \tag{9}$$

where M_{fin} is the water flow in the pipe, kg/s; $h_{\text{fin,in}}$ is the inlet enthalpy, kJ/kg; $h_{\text{fin,out}}$ is the outlet enthalpy, kJ/kg; k_{fin} is the fin heat transfer coefficient, W/m^2; A_{evap} is the fin heat exchange area, m^2; $t_{\text{fin,in}}$ is the intermediate inlet water temperature, ˚C; $t_{\text{fin,out}}$ is the intermediate outlet water temperature, ˚C.

Air side temperature change δt is

$$\delta t = \frac{3600 E_{\text{fin,evap}} \rho_{\text{air}}}{Q_{\text{air,in}} c_{\text{air}}}, \tag{10}$$

where ρ_{air} is the air density, kg/m^3; C_{air} is the air specific heat capacity, kJ/(kg·K).

5. System Operation Energy Consumption Model

Heating Seasonal Performance Factor (HSPF) [33] is the ratio of the heating capacity and the total power consumption of the heat pump unit in a specific area during the normal heating season. At the same time, considering the steady-state efficiency, environmental changes, and the power consumption of the equipment other than the compressor of the unit, the HSPFasp calculation formula of the heat storage heat pump unit is

$$\mathrm{HSPF}_{\mathrm{asp,PCM}} = \frac{\int_0^{\tau_{\mathrm{heat}}} q_{\mathrm{load}} \mathrm{d}\tau}{\int_0^{\tau_{\mathrm{unit}}} P_{\mathrm{asp}} \mathrm{d}\tau}. \tag{11}$$

The $\mathrm{HSPF}_{\mathrm{auxi}}$ calculation formula of the electric boiler combined heating unit is

$$\mathrm{HSPF}_{\mathrm{auxi}} = \frac{\int_0^{\tau_{\mathrm{heat}}} q_{\mathrm{load}} \mathrm{d}\tau}{\int_0^{\tau_{\mathrm{unit}}} P_{\mathrm{asp}} \mathrm{d}\tau + \int_0^{\tau_{\mathrm{boiler}}} P_{\mathrm{boiler}} \mathrm{d}\tau}, \tag{12}$$

where τ_{heat} is the heating time in heating season, h; τ_{unit} is the heating time of heat pump unit, h; P_{boiler} is the power of auxiliary electric boiler, kW; τ_{boiler} is the heating time of auxiliary electric boiler, h.

Due to the long-term operation in the sub-zero environment, the saturated air moisture content decreases significantly with the decrease of temperature, and frequent defrosting is required during the operation of the unit. However, frequent defrosting not only affects the heating effect of the unit, but also greatly affects the operating energy efficiency of the unit. The influence of defrosting on the actual heating effect of the unit is mainly reflected in the proportion of defrosting time x_1 and defrosting energy consumption x_2:

$$\begin{aligned} x_1 &= \frac{\tau_{\mathrm{def}}}{\tau_{\mathrm{heat}}}, \\ x_2 &= \frac{\int_0^{\tau_{\mathrm{def}}} P_{\mathrm{def}} \mathrm{d}\tau}{\int_0^{\tau_{\mathrm{heat}}} q_{\mathrm{load}} \mathrm{d}\tau}. \end{aligned} \tag{13}$$

The operation energy consumption of the electric boiler auxiliary air source heat pump system and the regenerative air source heat pump system is analyzed, mainly by comparing the primary energy consumption under the same outdoor working conditions and building load, and the low calorific value of standard coal($\mathrm{LHV}_{\mathrm{sc}} = 29.307$ MJ/kg) [34] is introduced for this purpose, and the primary energy consumption $\mathrm{PEC}_{\mathrm{EASP}}$ and utilization rate $\mathrm{PER}_{\mathrm{EASP}}$ of the electric boiler auxiliary heating system are

$$\begin{cases} \mathrm{PEC}_{\mathrm{EASP}} = \dfrac{3600}{\eta_E} \times \left(\dfrac{\int_0^{\tau_{\mathrm{unit}}} P_{\mathrm{asp}} \mathrm{d}\tau}{\eta_{\mathrm{asp}} \cdot \mathrm{LHV}_{\mathrm{sc}}} + \dfrac{\int_0^{\tau_{\mathrm{boiler}}} P_{\mathrm{boiler}} \mathrm{d}\tau}{\eta_{\mathrm{boiler}} \cdot \mathrm{LHV}_{\mathrm{sc}}} \right), \\ \mathrm{PER}_{\mathrm{EASP}} = \eta_E \cdot \eta_{\mathrm{asp}} \cdot \eta_{\mathrm{boiler}}. \end{cases} \tag{14}$$

$\mathrm{PEC}_{\mathrm{PASP}}$ and utilization rate $\mathrm{PER}_{\mathrm{PASP}}$ of the thermal storage air source heat pump system are

$$\begin{cases} \mathrm{PEC}_{\mathrm{PASP}} = \dfrac{3600 \times \int_0^{\tau_{\mathrm{unit}}} P_{\mathrm{asp}} \mathrm{d}\tau}{\mathrm{LHV}_{\mathrm{sc}} \cdot \eta_{\mathrm{asp}} \cdot \eta_E}, \\ \mathrm{PER}_{\mathrm{PASP}} = \eta_{\mathrm{asp}} \cdot \eta_{\mathrm{PCM}} \cdot \eta_E, \end{cases} \tag{15}$$

where η_E is the thermoelectric efficiency, 0.42.

6. Performance Comparison and Optimization of Heat Storage Heat Pump System and Electric Auxiliary Heat Pump System

A residential building with a heating area of 3000 m^2 in Dalian is selected as the main heating body. The building envelope, fresh air demand internal personnel, lighting, and other thermal disturbance factors are in accordance with the provisions of GB50189 "Energy-saving Design Standards for Public Buildings." The specific design parameters are shown in Table 1.

When the indoor temperature is maintained at 18°C, and the outdoor environment temperature changes from −15°C to 14°C, the scatter diagram of the change of building heat load with outdoor ambient temperature is obtained by using transient analysis software, as shown in Figure 4.

It can be seen from Figure 4 that the actual heat load of the building has an almost linear relationship with the outdoor temperature. When the outdoor temperature is 14°C, the building heat load is only 18 kW. With the decrease of outdoor temperature, the heat dissipation of the building gradually increases. When the outdoor temperature drops to −14°C, the maximum heat load of the building reaches 157 kW, at which time the heat demand of the building is the largest, and the heating capacity of the unit is the smallest. From the density of the scatter plot, it can be found that the concentration of building heat load is small in the area above 0°C. At this time, due to the small temperature difference between the inner and outer surfaces of the wall, the building heat dissipation is greatly affected by meteorological factors other than ambient temperature, such as solar radiation, rain, and snow. When the ambient temperature is lower than −10°C, the heat load distribution of the building is relatively concentrated. The heat loss of the building is mainly due to heat exchange with outdoor air in areas such as walls and windows. The influence of solar radiation on the heat dissipation of the building can be approximately ignored. The design of energy-saving buildings can also refer to this result and reduce the heating load of the building by installing double glazing and increasing the thickness of the insulation layer.

6.1. Performance Comparison between Heat Storage Heat Pump System and Electric Auxiliary Heat Pump System. Numerical simulation of the heating performance of the electric auxiliary heating air source heat pump system and the regenerative air source heat pump heating system is

Table 1: Building heat load design parameters.

Design parameter	
Heating system	Radiant floor heating
Supply and return water temperature/°C	45/35
Heat supply temperature/°C	18
Relative humidity/%	40
Building envelope	50% design standard for energy saving of public buildings
Number of occupants (person/m^2)	0.18
Room rate of personnel	0.7

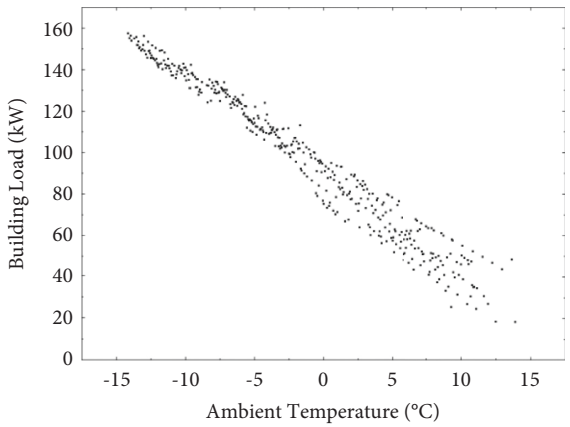

Figure 4: Distribution of building heat load with ambient temperature.

carried out in a typical meteorological year [26] in Dalian. Referring to the heating season time in Dalian, the simulation time was set from November 5 of the current year to April 5 of the next year, and in order to reduce the calculation amount and ensure the calculation accuracy, 1 h is taken as a time step. The simulation takes 1 h as a step. The sodium chloride solution with a mass concentration of 8.5% is selected as the phase change heat storage material. According to formula (6), the corresponding crystal phase transition point temperature of the sodium chloride solution of this concentration is −5°C. The change of HSPF of two heating methods with heating time in the heating season is shown in Figure 5:

It can be seen from the figure that the outdoor ambient temperature is high before the 1100 h of heating, that is, December 21, and the HSPF of the two heating methods is relatively close. After December 21, the outdoor ambient temperature decreases, and the heat storage heat pump system maintains the HSPF above 1.74 through heat storage and peak regulation. The average HSPF in the heating season is 2.24, while the minimum HSPF of the electric auxiliary heat pump system is 0.95, and the average heating HSPF in the heating season is 1.83. The HSPF of the electric auxiliary heat pump system is lower than 1 because the heating capacity of the unit is greatly attenuated under extremely cold conditions, and the electric boiler with lower thermal efficiency bears most of the night heat load.

Comparing the variation law of defrosting energy consumption with heating time of the two heating methods under frosting conditions, the results are shown in Figure 6.

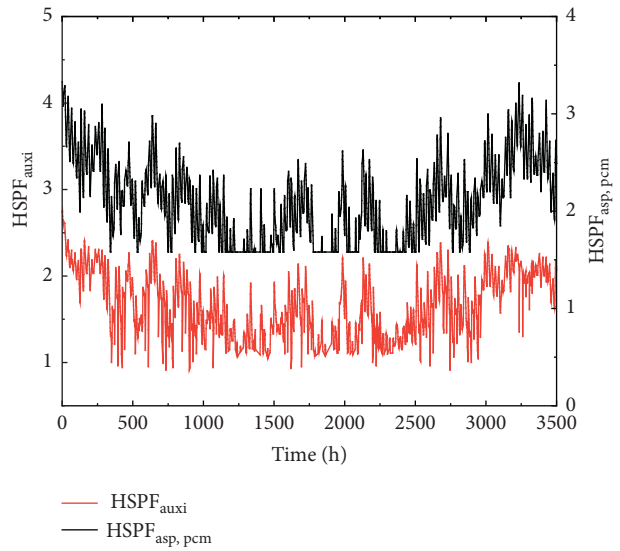

Figure 5: The change of HSPF of two heating methods.

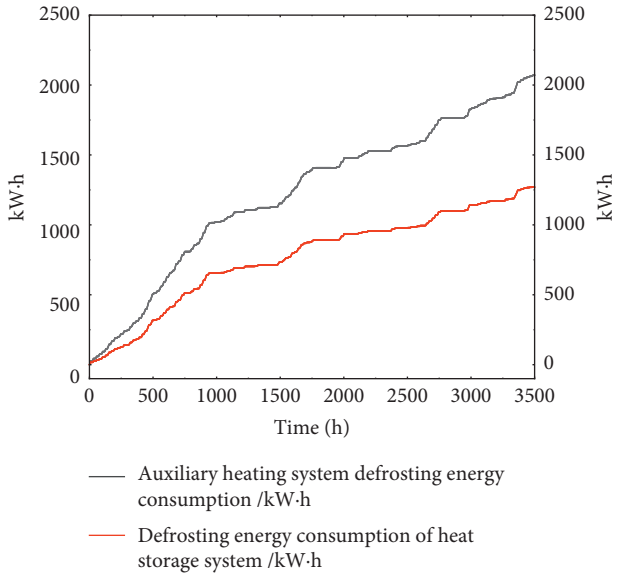

Figure 6: Comparison of defrosting energy consumption between two systems.

It can be seen from the figure that the defrosting energy consumption curves of the two heating methods have similar trends. In the period from 0 h to 1000 h, that is, from November 5 to December 17, the outdoor temperature hovered around 0°C, the outdoor air moisture content is

large, the frosting on the surface of the fin is fast and the frosting amount is large [35], and the defrosting energy consumption increases rapidly. And due to the short operating time of the heat storage device at this temperature, the defrosting energy consumption of the heat storage heat pump system is not significantly reduced. With the continuous decline of outdoor temperature and the decrease of air moisture content, the increasing trend of defrosting energy consumption of both systems is slowing down [35]. Due to the long-term operation of the heat storage device in the heat storage pump system under low temperature environment, the moisture content of the air is further reduced, and the frosting amount at the same time is reduced. In fact, the defrosting energy consumption of the system is less, and the difference between the defrosting energy consumption of the two systems is gradually enlarged. According to the simulation results, in the whole heating season, the defrosting energy consumption of the heat storage heat pump system is 1287 kW·h, and the total defrosting time is 330 h, accounting for 9.3% of the unit operating time. Compared with the electric auxiliary heat pump system, the defrosting energy consumption is reduced by 816 kW·h, and the defrosting downtime is reduced by 131 h. The simulation results show that the primary energy consumption of the heat storage heat pump system in the whole heating season is 47822kgcc, which saves 19.6% of the primary energy compared with the traditional electric auxiliary heat pump system.

6.2. Performance Optimization of Phase Change Heat Storage Air Source Heat Pump System. In order to further optimize the performance of the heat storage air source heat pump system and analyze the actual energy consumption performance of the system, adjust the concentration of sodium chloride salt in the heat storage device appropriately. The temperature of the phase transition point of the heat storage device is changed with a step size of 1°C, and the change of HSPF and the primary energy consumption of the system under different temperatures are obtained as shown in Figure 7. The cumulative heat storage and defrosting energy consumption in the heating season are shown in Figure 8.

According to Figure 7, the HSPF of the heat storage heat pump system shows a trend of first increasing and then decreasing with the decrease of the heat storage temperature, and the primary energy consumption is the opposite. Although the energy efficiency ratio of the heat pump unit increases with the increase of the intake air temperature after preheating, it can be seen from Figure 8 that, with the increase of the phase transition point temperature, the accumulated heat storage in the heating season also increases. Due to the mechanical loss in the heat storage process of the heat storage device, and the heat loss in the heat storage and heat release process, the increase of the HSPF of the unit with the increase of the phase transition point temperature has a certain limit. The heat loss from heat storage caused by the excessive high phase transition point temperature is greater than the electric energy saved by the improvement of the unit efficiency. When the phase transition point temperature

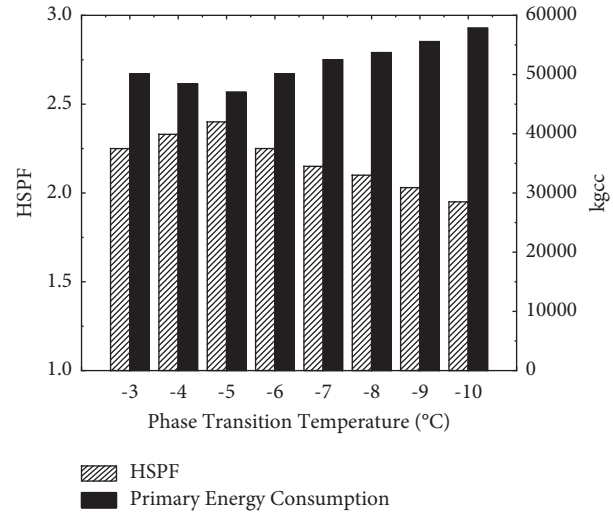

Figure 7: HSPF and primary energy consumption at different phase transition temperature.

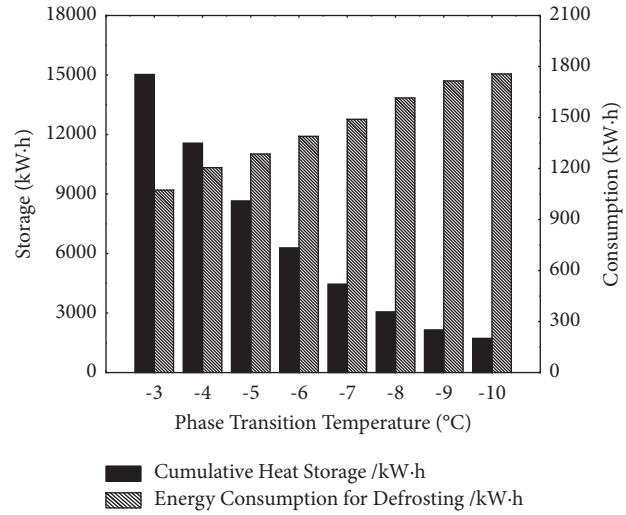

Figure 8: Cumulative heat storage and defrosting energy consumption at different phase transition point temperatures.

is −5.9°C, the system has a maximum HSPF of 2.33, and the primary energy consumption is 45736kgcc, which is 23.2% less than the electric auxiliary heat pump system. The defrosting energy consumption of the unit decreases with the decrease of the phase transition point temperature, and the decreasing trend gradually slows down. The analysis is because the low temperature air has a low moisture content. When the air temperature is lower than −9°C, the amount of frost itself is very small, and the amount of frost that is reduced by thermal storage preheating does not account for a small proportion of the total amount of frost.

7. Conclusion

(1) When the sodium chloride solution with a mass concentration of 8.5% is used as the phase change heat storage material, the average HSPF of the phase change heat storage air source heat pump system in

the heating season is 2.24, which is 0.41 higher than that of the traditional electric auxiliary heat pump system. The primary energy consumption is 47852kgcc, the defrosting energy consumption is 1287 kW·h, which are 19.6% and 38.8% lower than those of the electric auxiliary heat pump system respectively, and the defrosting downtime is reduced by 28.4%.

(2) When the sodium chloride solution with a mass concentration of 10% is used as the phase change heat storage material, the phase change heat storage heat pump system has the best system operation economy, and the average HSPF in the heating season of the system reaches 2.33, which reduces the defrosting energy consumption by 34% and saves primary energy by 23.2% compared with the traditional electric auxiliary heat pump system under the same working conditions.

(3) The regenerative air source heat pump system using sodium chloride solution as the low-temperature phase change heat storage material operates stably, which can significantly reduce the energy consumption of defrosting and heating.

(4) Due to the limitation of compressor capacity and noise problem, air source heat pump cannot be large-scale. When heating in large areas, dozens of units are generally used in parallel. When the number of parallel units is too large, or the spacing is too small, the mutual interference between suction and exhaust between units is likely to occur, resulting in obvious cold island effect [36]. At this time, even at a high outdoor temperature, the evaporation temperature of the unit in the middle position will also decrease sharply, resulting in the performance degradation of the unit. The numerical simulation in this paper relies on the mathematical model of a single unit, which cannot analyze the operating characteristics when multiple units are operated in parallel. Therefore, the existing mathematical model needs to be improved in the next step to increase the interference the interference component between different units for large-scale heating in order to investigate the energy saving performance of the system when applied to large-scale regional heating.

Data Availability

The data used to support the findings of this study are available from the corresponding author upon request.

Disclosure

The funders had no role in the design of the study; in the collection, analyses, or interpretation of data; in the writing of the manuscript, or in the decision to publish the results.

Conflicts of Interest

The authors declare no conflicts of interest.

Authors' Contributions

Ronghua Wu and Caihong Yin conceptualized the study. Caihong Yin developed the methodology. Hao Zhan and Hao Yu provided the software. Ronghua Wu and Caihong Yin performed validation. Changqing Liu performed formal analysis. Hao Zhan wrote the original draft. Caihong Yin and Ronghua Wu reviewed and edited the article and did funding acquisition. All authors have read and agreed to the published version of the manuscript.

Acknowledgments

This research was funded by Qingdao Citizens' Health Science and Technology Plan Project "Low-grade Energy Heating and Cooling Technology and Application Demonstration" (Project No.: 19-6-1-79-nsh) and National Natural Science Foundation of China Youth Project "Viscoelastic Pipeline Hydraulic Transient Dynamic Behavior and Fluid-Structure Interaction Mechanism Research"(-Project No.: 51808102).

References

[1] J. Cho, B. Park, and T. Lim, "Experimental and numerical study on the application of low-temperature radiant floor heating system with capillary tube: thermal performance analysis," *Applied Thermal Engineering*, vol. 163, Article ID 114360, 2019.

[2] F. Qin, Q. Xue, G. Albarracin Velez, G. Zhang, H. Zou, and C. Tian, "Experimental investigation on heating performance of heat pump for electric vehicles at −20 °C ambient temperature," *Energy Conversion and Management*, vol. 102, pp. 39–49, 2015.

[3] W. Ji, B. Dq, N. A. Long, and Y. Yang, "Experimental study on an injection-assisted air source heat pump with a novel two-stage variable-speed scroll compressor-Science Direct," *Applied Thermal Engineering*, vol. 176, 2020.

[4] A. Lx, A. El, A. Yx, M. Ning, S. Xi, and W. Xinlei, "An experimental energy performance investigation and economic analysis on a cascade heat pump for high-temperature water in cold region," *Renewable Energy*, vol. 152, pp. 674–683, 2020.

[5] W. Wu, C. Zhai, S. M. Huang, Y. Sui, Z. Sui, and Z. Ding, "A hybrid H2O/IL absorption and CO2 compression air-source heat pump for ultra-low ambient temperatures," *Energy*, vol. 239, Article ID 122180, 2022.

[6] H. Zhang, X. Geng, S. Shao, S. Chunqiang, and W. Zhichao, "Performance Analysis of a R134A/CO_2 cascade Heat Pump in Severe Cold Regions of China," *Energy*, vol. 239, 2022.

[7] M. Wang, Y. Cheng, and J. Yu, "Analysis of a dual-temperature air source heat pump cycle with an ejector," *Applied Thermal Engineering*, vol. 193, Article ID 116994, 2021.

[8] J. Sager and J. P. Poirier, "Assessing the Performance and Cost-Competitiveness of a Dual-Source Solar Assisted Heat Pump in Cold climates," *E3S Web of Conferences*, vol. 246, 2021.

[9] Y. Sun, S. Liu, Y. Liu et al., "Study on optimal operation of boiler-assisted air source heat pump heating system," *Journal of Physics: Conference Series*, vol. 2185, no. 1, Article ID 012071, 2022.

[10] R. Zhao, Y. Liu, C. Li, and B. Wang, "An Energetic, Economic and Environmental Evaluation of a Dual-Source Heat Pump

Water Heater–A Case Study in Beijing," *Energy Conversion and Management*, vol. 253, 2022.

[11] S. Ji, Y. Liu, H. Xu, and Y. Yiwei, "Application and Analysis of Air-Source Heat Pump Heat Supply System in Cold Areas," in *Proceedings of the 2021 International Conference on Applied Physics and Energy Development*, Bristol, UK, 2022.

[12] H. Chen, Y. Wang, and J. Li, "Experimental research on a solar air-source heat pump system with phase change energy storage," *Energy and Buildings*, vol. 228, 2020.

[13] B. Zhang, J. X. Cai, and W. H. Zhou, "Solar Energy Coupling Air Source Heat Pump System Based on Preheating Cold Air," *Building Energy Efficiency*, vol. 40, 2012.

[14] W. Xu, C. Liu, A. Li, and J. Li, "Feasibility and Performance Study on Hybrid Air Source Heat Pump System for Ultra-low Energy Building in Severe Cold Region of China," *Renewable Energy*, vol. 146, 2020.

[15] Y. Tao and Y.-L. He, "A review of phase change material and performance enhancement method for latent heat storage system," *Renewable and Sustainable Energy Reviews*, vol. 93, pp. 245–259, 2018.

[16] H. Wang, M. Xiaomeng, Z. Liugang, X. Zhang, Y. Mei, and A. Zhang, "Numerical and experimental study of effect of paraffin phase change heat storage capsules on the thermal performance of the solar pond," *Energy Exploration & Exploitation*, vol. 39, no. 3, pp. 1010–1023, 2021.

[17] X. Huo, D. Xie, Z. Zhao, W. Shujun, and M. Fanbin, "Novel Method for Microencapsulation of Eutectic Hydrated Salt as a Phase Change Material for thermal Energy storage," *International Journal of Low-Carbon Technologies*, vol. 17, 2022.

[18] R. Sidqy, A. S. Pamitran, D. A. Setiadi, and P. P. Mufti, "Seawater Ice Slurry for Shrimp Cooling Using Scraper Blade Ice Slurry generator," in *Proceedings of the AIP Conference Proceedings*, 2020.

[19] D. W. Lee and J. B. Kim, "Characteristic analysis of the cooling system using ice slurry type heat storage system," *Journal of Energy Engineering*, vol. 20, no. 1, pp. 30–35, 2011.

[20] Sasaki, "Ice slurry and latent heat storage," *Distribution Refrigerators*, vol. 90, pp. 277–281, 2015.

[21] M. Song, S. Deng, C. Dang, N. Mao, and Z. Wang, "Review on improvement for air source heat pump units during frosting and defrosting," *Applied Energy*, vol. 211, pp. 1150–1170, 2018.

[22] K. Sezen and A. Gungor, "Performance analysis of air source heat pump according to outside temperature and relative humidity with mathematical modeling," *Energy Conversion and Management*, vol. 263, Article ID 115702, 2022.

[23] S. Huang, W. Zuo, H. Lu, C. Liang, and X Zhang, "Performance comparison of a heating tower heat pump and an air-source heat pump: a comprehensive modeling and simulation study," *Energy Conversion and Management*, vol. 180, pp. 1039–1054, 2019.

[24] X. Guo, Y. J. Wang, and B. Yang, "Numerical simulation of dynamic characteristics of R410A heat pump air conditioner under frost condition," *Low Temperature and Superconductivity*, vol. 6, no. 4, 2010.

[25] M. Yu, *Characteristics of Direct Phase Change Heat Storage Air Source Heat Pump and its Application in Severe Cold regions*, Zhejiang University, Zhejiang, China, 2021.

[26] L. Zhang, Y. Jiang, and J. Dong, "An experimental study of frost distribution and growth on finned tube heat exchangers used in air source heat pump units," *Applied Thermal Engineering*, vol. 132, pp. 138–151, 2018.

[27] M. L. Qu, R. Zhang, T. Y. Zhang, and F. Zhang, "Experimental study on energy consumption of defrosting by phase change energy storage of cascade air source heat pump," *Journal of Refrigeration*, vol. 40, no. 4, pp. 23–28, 2019.

[28] M. Song, D. Chaobin, M. Ning, and D. Shiming, "Energy transfer procession in an air source heat pump unit during defrosting with melted frost locally drainage in its multi-circuit outdoor coil," *Energy and Buildings*, vol. 164, pp. 109–120, 2018.

[29] X. Liu, Y. Li, K. Zhuang, R. Fu, S. Lin, and X Li, "Performance study and efficiency improvement of ice slurry production by scraped-surface method," *Applied Sciences*, vol. 9, no. 1, p. 74, 2018.

[30] T. Sharma and P. Kalita, "Modeling and Simulation of Phase Change Process in Ice Thermal Energy Storage," in *Proceedings of the COMSOL International Conference*, Bangalore, India, 2018.

[31] L. Z. Song, S. C. Liu, and Z. M. Rao, "Experimental study on sodium chloride ice slurry system," *Fluid Machinery*, vol. 41, no. 10, pp. 65–68, 2013.

[32] S. Mi, L. Cai, K. Ma, and Z. Liu, "Investigation on flow and heat transfer characteristics of ice slurry without additives in a plate heat exchanger," *International Journal of Heat and Mass Transfer*, vol. 127, pp. 11–20, 2018.

[33] S. Kim, Y. Jeon, H. J. Chung, and Y. Kim, "Performance optimization of an R410A air-conditioner with a dual evaporator ejector cycle based on cooling seasonal performance factor," *Applied Thermal Engineering*, vol. 131, pp. 988–997, 2018.

[34] M. Jarre, M. Noussan, and M. Simonetti, "Primary energy consumption of heat pumps in high renewable share electricity mixes," *Energy Conversion and Management*, vol. 171, pp. 1339–1351, 2018.

[35] R. Mao, Y. Yang, P. Pei et al., "Research on the frosting rule and frost suppression strategy of air source heat pump in guiyang, China," *IOP Conference Series: Earth and Environmental Science*, vol. 495, no. 1, Article ID 012006, 2020.

[36] B. Rogié, J. Kjær Jensen, S. Ole Kjøller Hansen, and W. Brix Markussen, "Analysis of cold air recirculation in the evaporators of large-scale Air-source heat pumps using CFD simulations," *Fluid*, vol. 5, no. 4, p. 186, 2020.